4

Proton Density of Tissue Water[1]

Paul Tofts

Department of Medical Physics, NMR Research Unit, Institute of Neurology, University College London, Queen Square, London WCIN 3BG, UK

4.1 INTRODUCTION

Proton density (PD) refers to the concentration of protons in tissue, protons being the hydrogen nuclei that resonate and give rise to the NMR signal. Since most visible tissue protons are resident in water, it is often seen as a short-hand way of looking at water content, although the proton concentration in lipid, where present, is also high. PD is often expressed as a percentage of the proton concentration in water (thus CSF is 100 pu[2] and white matter is about 70 pu).

All images have intensity proportional to PD (if the number of protons in a voxel is halved,

[1] Reviewed by Dr Alex Mackay.

[2] It is recommended that PD is expressed in percentage units (pu), to avoid the confusion that can arise when using percentages. Magnetization transfer ratio (MTR) is also often expressed in pu, for the same reason (see Chapter 8).

Quantitative MRI of the Brain. Edited by Paul Tofts
 ISBN: 0-470-84721-2

the signal will halve). Images with very little T_1 or T_2 weighting are often called 'PD-weighted'; however all images have intrinsic PD weighting, in addition to any dependence on other parameters such as T_1, T_2 or diffusion. Thus the influence of changes in PD is always implicitly present. In principle, PD is measured from the image intensity in the absence of any T_1 or T_2 losses; practicalities may prevent this from being possible, and suitable corrections for T_2, and sometimes T_1, losses are usually made. To obtain absolute values of PD, a concentration standard is needed (as it is for absolute metabolite concentration measurements in spectroscopy, as discussed in Chapter 9). To obtain accurate measurements, the nonuniformity of the RF field must be taken account of, particularly at higher static (B_0) fields.

So called 'PD-weighted' images are used extensively in radiology.[3] Ideally these should have a short *TE* (to minimize T_2 losses), and a long *TR* (to minimize T_1 losses). In practice these usually have an echo time, *TE*, of 20–30 ms, and a repetition time, *TR*, of 2–5 s;[4] thus there is significant T_2-weighting,[5] and often significant T_1-weighting, in addition to the PD weighting. In fact when a lesion is seen as bright in such an image, it is unclear how much of the visible contrast derives from a PD increase and how much from a T_2 increase.[6]

PD is sometimes called 'spin density', as the protons are functioning as spins in the magnetic fields. It is sometimes abbreviated as N(H) (referring to the number of hydrogen nuclei) or ρ (to denote spin density). Since only protons with

[3] In some clinical departments they are being replaced by fast FLAIR (which detects more lesions).

[4] In multiple sclerosis (MS), the *TR* is deliberately shortened down to about 2 s (at 1.5 T), in order to reduce the signal from CSF $T_1 \approx 4$ s), and increase the conspicuity of periventricular lesions. Thus the SE2000/30 sequence, nominally PD-weighted for lesions, is actually T_1-weighted for CSF. T_1 and T_2 weighting are discussed more in Chapters 5 and 6.

[5] The T_2 of grey and white matter proportional to 90 ms (at 1.5 T); this gives a signal loss of 20 % at $TE = 20$ ms. In contrast, a lesion with $T_2 = 200$ ms (as often seen in MS; Stevenson *et al*., 2000) will only suffer 10 % loss, thus appearing 10 % brighter than normal tissue (although T_1 losses might reduce this factor a little).

[6] Although recent work suggests that MS lesions have a substantially higher PD (Laule *et al*., 2002), and the water content of MS lesions (measured post-mortem) is substantially raised (see Section 4.6).

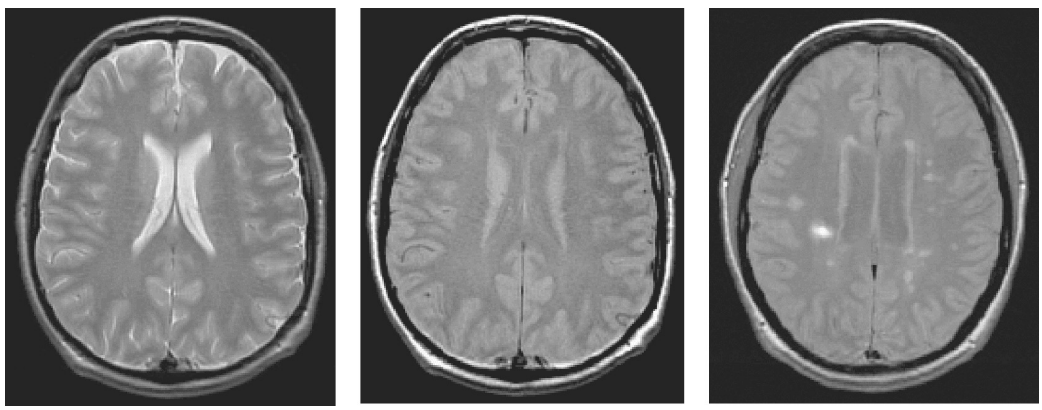

Q1 **Figure 4.1.** •PD-weighted images (fast spin echo, $TE = 19$ ms). With long *TR* (12 s) the CSF is nearly fully relaxed ($T_1 = 4$ s), and appears bright (PD = 100 pu), followed by grey matter (PD = 82 pu) and white matter (PD = 70 pu). To reduce the CSF signal nearly down to the level of the white matter, *TR* can be reduced to 2 s. In a person with MS, lesions are then visible, even near the ventricles at $TR = 12$ s, the CSF signal is 5 % saturated (see Figure 4.9), but the other tissues are completely relaxed. The left-hand image looks similar to a conventional T_2-weighted image, which also has bright CSF (because of its long T_2) and grey matter brighter than white matter (because of its higher PD). The normal images are those of the author, PT

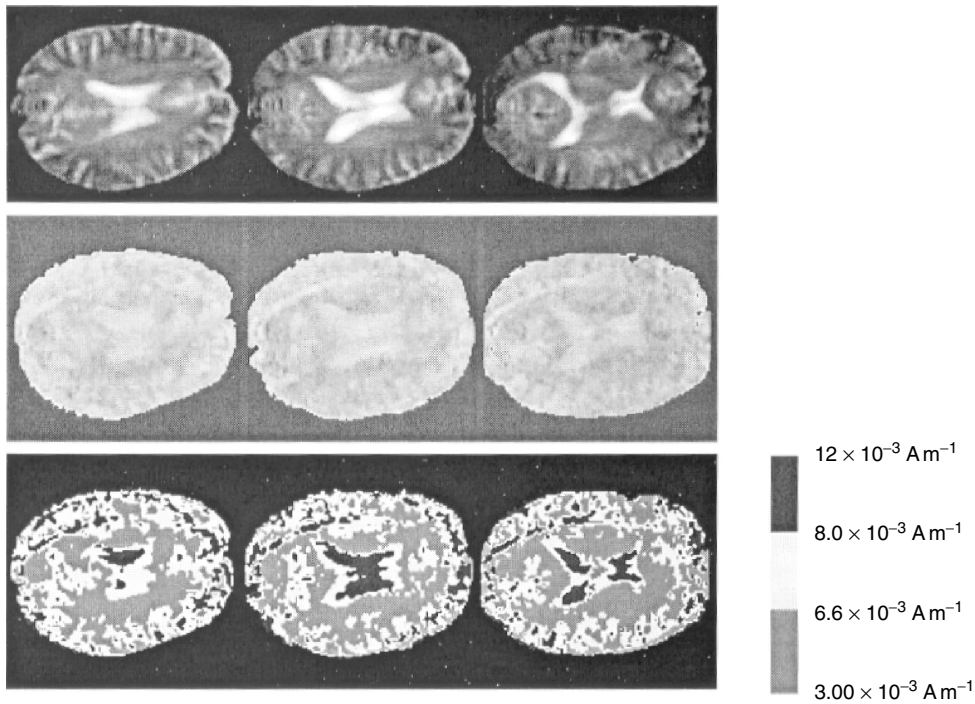

Q1 **Figure 4.2 (Plate 2).** •Proton density measured using the distant dipolar field (DDF) method. Top row, conventional images; middle row, PD map; bottom row, colour-coded PD map, with colour scale chosen to segment CSF, grey matter and white matter. Reproduced from Gutteridge, S., Ramanathan, C. and Bowtell, R. 2002, Mapping the absolute value of M_0 using dipolar field effects, in *Magn. Reson. Med.*, Copyright 2002. This material is used by permission of Wiley-Liss Inc., a subsidiary of John Wiley & Sons Inc.

$TE \geq 10$ ms are included in the measurement (thus excluding the large number of lipid protons; see below), it should be born in mind that PD (as measured by MRI) is actually 'mobile proton density', 'free PD', or water proton density, not total proton density. Some workers have measured 'relative proton density' (Brix *et al.*, 1990; Roberts *et al.*, 1996). This term must be treated with caution, as it can mean the fraction of protons in a particular pool (relative to the total number of protons) or the PD relative to other tissues in the same slice or the PD relative to a standard such as water.

The biological location of the protons is an intriguing question that many have addressed. It is now thought that the MRI-visible protons are all in water, that there is no pool of MRI-invisible bound water, and that there is also a large pool of MRI-invisible short-T_2 nonaqueous protons, primarily located in lipid, proteins and cellular structures; in white matter this constitutes 30 % of the total protons. Thus MRI PD sees only water protons.

PD measurement scan be used to infer water content, its change in disease (oedema), and its response to treatment (e.g. mannitol to reduce oedema). PD maps are also used to aid multispectral segmentation and tissue classification schemes, in conjunction with T_1, T_2 and sometimes diffusion maps.

Proton density

Proton density, or spin density, refers to the concentration of MRI-visible protons (hydrogen nuclei) in tissue. Most are located in water,

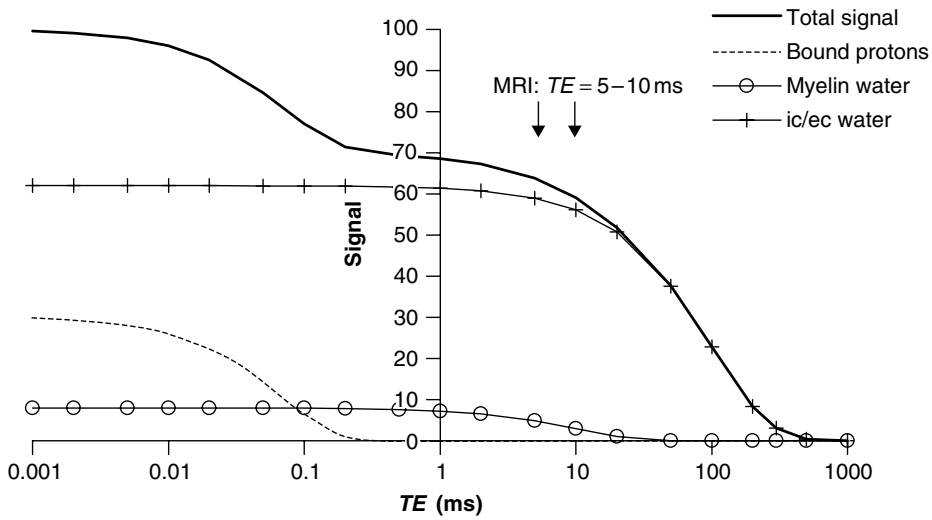

Figure 4.3. Symbolic illustration of tri-exponential decay of transverse proton signal in white matter. In this computer simulation, using realistic pool-sizes and T_2-values, 30 % of the protons are nonaqueous and bound ($T_2 = 70$ μs), 8 % are water protons trapped in myelin ($T_2 = 10$ ms), and 62 % are in intra- and extracellular (ic/ec) water. The bound protons are MRI-invisible; the myelin water protons are partly MRI-visible, for sequences with $TE = 5–10$ ms. MRI acquisition at several echo times greater ($TE \geq 5–10$ ms) enables the full myelin water signal to be recovered, in the presence of the decaying ic/ec signal

and virtually all tissue water is visible provided a short *TE*, long *TR* acquisition is used. There is also a large pool of bound nonaqueous protons (30 % of protons in white matter) that is MRI-invisible. The measured proton density depends on the echo time used (see Figure 4.3)

Increases in PD correspond largely to oedema, and reduction in PD can be seen after treatment. Changes in PD often correlate closely with T_1 changes, and may provide no extra information, if T_1 has already been measured.

Measurement of PD requires multiecho acquisition, usually at long repetition time, and is time-consuming. Suitable correction for RF nonuniformity is usually required. PD measurement is not yet carried out routinely. New more efficient sequences are proposed.

Water trapped in myelin has been identified in white matter; it is greatly reduced in grey matter and in MS (as a result of demyelination).

4.2 PHYSICAL BASIS OF PROTON DENSITY

4.2.1 Proton Concentration

The absolute proton concentration [^{1}H] or PC of a tissue defines the number of protons per unit volume of tissue. For a chemical compound of known composition, the concentration is:

$$\mathrm{PC} = \mathrm{NP}\rho/\mathrm{MWt\ M} \qquad (4.1)$$

where NP is the number of protons per molecule, ρ is the density (g l^{-1}), MWt is the molecular weight, and the units of concentration are molar. Thus water has a proton concentration PC = 110.4 M (NP = 2; $\rho = 0.9934$ g l^{-1} at 37 °C; MWt = 18) at body temperature, and a slightly higher value at room temperature. This is twice the concentration or molarity of pure water (55.2 M), since there are two protons in each molecule of water. The signal is proportional to PC (for more discussion of other factors, see below).

Table 4.1. PD values in normal tissue[a,b]

Reference	White matter	Grey matter
Wehrli *et al.* (1985)[c]	77 (SEM = 5)	86 (SEM = 5)
Whittall *et al.* (1997)[d]	71 (SEM = 2)	83 (SEM = 2)
Farace *et al.* (1997)[e]	69 (SEM = 2)	82 (SEM = 3)
Gutteridge *et al.* (2002)[f]	70 (SEM = 1)	78 (SEM = 1)

SEM = standard error of the mean = standard deviation/$\sqrt{(\text{no. of observations})}$.
[a]In pu (percent units; water = 100 pu).
[b]No attempt to extract regional variations has been made, although these must be present. The grey matter values may be subject to partial volume errors with CSF and white matter.
[c]Early work. CSF was used an internal standard; no correction was made for RF nonuniformity. Note the large SEM values.
[d]Multiecho analysis method of Mackay and Whittall. Several locations of white matter and of grey matter have been averaged together. Myelin water fractions were 11 % (white matter) and 3 % (grey matter). Correction for the temperature of the water concentration standard attached to the head would raise the PD estimates by up to 3–4 pu, depending on its temperature.
[e]Bags of water around the head were used as concentration standards. Temperature correction would raise PD estimates by 3–4 pu.
[f]DDF method – see Figure 4.2 and (Plate 2) Section 4.4.1. Voxel size 3 × 3 × 7 mm.

4.2.2 Proton Density

The proton density PD of a tissue usually refers to the concentration of protons in the tissue, relative to that in the same volume of water at the same temperature. Thus:

$$\text{PD} = \text{PC}/1.104 \text{ pu} \tag{4.2}$$

where PC is in M, and PD is in pu. Thus pure water or CSF has PD = 100 pu, and white matter has PD $\approx$ 70 pu. Typical values for PD are shown in Table 4.1.

4.2.3 Measuring PC or PD

Measuring PC or PD is usually carried out using a sequence with minimal T_1 or T_2 weighting; the residual weighting is removed using an analytic model for the signal intensity. The signal intensity of a spin echo sequence is usually modelled by:

$$S = g \text{ PD}[1 - \exp(-TR/T_1)] \exp(-TE/T_2) \tag{4.3}$$

where g is the signal from tissue with unit PD in the absence of T_1 or T_2 losses (i.e. long repetition time, TR, short echo time, TE); g can be thought of as the gain of the receiver system. It defines the relationship between PD and the resulting signal, in the absence of relaxation time losses (a similar expression can be written for PC). Thus by measuring the signal for several TE values (including a short one), the signal at $TE = 0$ can be inferred from this model. By measuring the signal at several TR values, including a long one, the fully relaxed signal (for $TR = 4$) is inferred [again assuming Equation (4.3) is an adequate model]. By combining these two analyses, the signal at $TE = 0$ and $TR = 4$ can be estimated. This is g PD. By measuring the signal for a substance with known PD (usually water[7]), g can be found. The signal from a tissue with unknown PD (e.g. white matter) then gives its PD value. If required, PC can be calculated using Equation (4.2). Note that we have assumed all the protons have long enough T_2 to be seen by the imaging process, that the spin echo sequence has perfect 90 and 180° pulses, and that g does not depend on position. These issues will be discussed in detail in Section 4.6.

[7] If the temperature of the water standard is different from body temperature, this must be taken into account; see Section 4.4.

4.2.4 MRI Visibility

Some protons may be MRI-invisible. Protons with a T_2 longer than about 10–30 ms are seen in the spin echo[8], although their signal may still be reduced, depending on the T_2 value. These are said to be MRI-visible. Protons with shorter T_2s suffer signal loss, and below about 5 ms are effectively invisible to the imaging process. They can, however, be seen using a spectrometer with short pulses and no echoes; components with T_2 as low as 20–50 μs have been seen in fixed white matter (Ramani *et al*., 2001; Brix *et al*., 1990). Thus when we talk about proton density, the value we measure depends on the minimum echo time used; the lower this is, the higher the PD that will be measured, as the short-T_2-bound components become increasingly visible (see Figure 4.3).

4.2.5 Water Content

Pathologists and surgeons have measured water content for many decades, using biopsy or post-mortem tissue. Although water content is intrinsically different from proton density, its measurement gives some confirmation that changes in PD measured in disease are approximately correct, and values are remarkably similar, particularly in white matter (see Tables 4.1 and 4.2). Nonetheless, there are two principle reasons why the value of water content can, in principle, differ from free PD (i.e. PD measured with MRI).

First, water content will potentially include bound water that has a short T_2 and is MRI-invisible (and hence excluded from the PD measurement). In earlier determinations of water content, based on weight loss on evaporation (Tourtellotte and Parker, 1968; Norton *et al*., 1966), the sample was heated, sometimes *in vacuo*, until its mass did not change any more. This 'dry weight' was subtracted from the original 'wet weight' to give the water content as a mass fraction. Thus the measured 'water content' could depend on the temperature to which the sample had been heated (since more bound water may be evaporated off at higher temperatures). Faster determinations (Takagi *et al*., 1981; MacDonald *et al*., 1986) have used the 'gravimetric method' (Marmarou *et al*., 1978; Nelson *et al*., 1971); the sample is floated in a gradient column made up of a layered mixture of organic solvents of known density. A previous measurement of the solids content in normal brain tissue is then used to infer the water content of the sample. It is also possible to identify distinct water compartments, based on whether the water is freezable or not, using differential scanning calorimetry (Kaneoke *et al*., 1987; see Table 4.2). The freezable water is thought to be relatively free, whilst the unfreezable water is relatively bound, although how this relates to free and bound protons (as defined by their T_2 values) is unclear. Water content is usually measured in units of grams water per gram tissue, and thus it will differ slightly from PD, because of the slightly different densities of brain tissue and water. Thus the measured value of water content is potentially greater than free PD, since some bound (short T_2) water (if present) could be included.

Secondly, there are significant numbers of protons that are resident in nonwater environments (e.g. lipids or macromolecules), although most of these have short T_2s and are therefore MRI-invisible. Spectroscopy in normal brain shows no lipid peak, thus the lipid protons are relatively bound, with a short T_2, and probably make little contribution to PD in most brain tissues.[9] This phenomenon could make water content smaller than PD.

4.2.6 Does Free PD Equal Water Content?

The effect of the two factors discussed above seems to be small in practice, and the normal values for water content and PD are very close, at least in white matter (Tables 4.1 and 4.2). Two of the PD values should probably be raised by about 3 pu to account for the temperature of the concentration standard. Thus the mean PD value

[8] Depending on the minimum *TE*. Exponential fitting to multi-echo data will recover most of this lost signal (see 'myelin water estimation' in Section 4.4.1).

[9] Low concentrations of free lipid are seen in spectra of MS lesions (Davie *et al*., 1993).

Table 4.2. Post-mortem and biopsy determinations of water content (percentage weight)[a] in normal brain tissue

Reference	White matter	Grey matter
Norton *et al*. (1966)[b]	71.6 (SEM = 2.2)	81.9 (SEM = 0.5)
Tourtellotte and Parker (1968)[c]	70.6 (SEM = 1.2)	Not measured
Schepps and Foster (1980)[d]	69	80
Takagi *et al*. (1981)[e]	70.4 (SEM = 0.2)	84.7 (SEM = 0.2)
Kaneoke *et al*. (1987)[f]	68 (SEM = 3)	Not measured
Bell *et al*. (1987)[g]	69.7 (SEM = 0.7)	80.5 (SEM = 0.8)
Fatouros and Marmarou (1999)[h]	68.7–69.6 (SEM = 0.2)	Not measured

[a]To convert water content values (g water/g tissue) to PD values, multiply by the specific gravity of brain tissue (1.04 for both white and grey matter; Whittall *et al*., 1997; Takagi *et al*., 1981; Torack *et al*., 1976). To convert to proton concentration (PC), multiply by the specific gravity and by the molarity of water (55.2 M); thus a water content of 71 pu is 40.6 M. To obtain the PC in μmol g^{-1}, multiply the water content by 55.2 (thus a water content of 71 pu is 39.2 μmol g^{-1}).

[b]Evaporation technique in three subjects. Lipid contents were: white matter, 15.6 pu (SEM = 0.3 pu); grey matter, 5.92 pu (SEM = 0.03 pu).

[c]Evaporation technique in 10 subjects. Lipid content of white matter was 18.7 pu (SEM = 0.4 pu). Others have reported lipid contents for white matter 16.1 pu, grey matter 6.3 pu (Brooks *et al*., 1980).

[d]Samples were dried to constant weight at 105 °C. Estimated from published percentage volume figures (74 % and 84 %), and solid fraction density = 1.3 g ml^{-1}.

[e]Gravimetric analysis in at least five subjects (37 samples). SD = 0.5 pu. SEM estimated.

[f]Samples dried to 200 °C. Differential scanning calorimetry measured the freezable water fraction; a bound (unfreezable) water fraction of 17.5 ± 3 % of the total water content was identified.

[g]Gravimetric determination from biopsy samples (12 of grey matter, nine of white matter).

[h]From T_1 values in 27 subjects [see Equation (4.4)]. The first figure is frontal white matter, the second is posterior white matter.

is about 73 pu in white matter. The water content values have to be multiplied by the specific gravity to give comparable volume concentrations, which average 72.5 pu.

Whittall *et al*. (1997) argue convincingly that all the tissue water is visible in their multiecho technique (MacKay *et al*., 1994; the water having a T_2 of at least 10 ms), that there is no pool of MRI-invisible water, that all the nonaqueous proton signal decays to zero in <1 ms, and that therefore PD measured in this way is in fact equal to the water content (see also Stewart *et al*., 1993). The ratio of myelin water fractions, between white matter and grey matter, measured using the multiecho MRI method of Mackay and Whittall (Table 4.1, 11 and 3 %) is comparable with the ratio of lipid fractions measured post-mortem by Norton (Table 4.2, 16 and 6 pu).

In a series of autopsy samples from grey and white matter (Fischer *et al*., 1990), multiecho data were collected at intervals of 2.3 ms. It was found that measured MRI signal amplitudes (extrapolated back to $TE = 0$, and corrected for receiver gain, i.e. proportional to PD), correlated much better with water content than with estimated proton content (taking into account bound protons). Fischer concluded that myelin lipids do not contribute to the signal (citing the lack of a lipid peak in normal brain spectra).

Some spectroscopists (Christiansen *et al*., 1994; Ernst *et al*., 1993; Kreis, 1997) have argued that PD measurements miss some bound water. In his review (Kreis, 1997), Kreis states that 'the water content determined by MR methods is well below the generally accepted values obtained by invasive methods, because a certain fraction of the total cerebral water signal has very short T_2 and usually escapes detection'. Ernst *et al*. (1993) measured values of PD 8–11 pu lower than published water content values, using a minimum $TE = 30$ ms.

Consideration of myelin water with a $T_2 = 13$ ms, and other corrections, led to final values only 2–3 pu below those determined biochemically. The authors concluded 'the concept of a pool of NMR-invisible water does not have to be invoked if all corrections are valid'. Christiansen *et al.* (1994) measured PD values using spectroscopic volumes of $2 \times 2 \times 2$ cm, and found values about 4 pu below those expected, given the grey/white fractions in the voxel, and published values of water content. However a monoexponential fit to signals at *TE*s of 20, 46, 92 and 272 ms was used, so it is likely that some of the myelin water ($TE = 10$–50 ms) was missed. Danielsen *et al.* (1994) measured an average brain water content of 68.5 pu, using $2 \times 2 \times 2$ cm voxels, primarily in white matter. This value is close to the invasively measured values of white matter water content (71 pu; Table 4.2). The minimum echo time was 20 ms, and no short T_2-component was included in the fitting, so unseen myelin water could again account for this discrepancy. Most workers have failed to take account of the decrease in magnetization and signal, as water is warmed from room temperature to body temperature (see Section 4.4); this effect (about 6 %, i.e. 4 pu for white matter) could account for much of the reported discrepancy.

In summary, the free PD probably does correspond to the all the protons in water, and no other protons, provided the short-T_2 myelin water has been included in the PD estimation.

4.2.7 Water Compartments in Neural Tissue

Several workers have observed multiple water compartments in neural tissue, using multiexponential analysis of transverse magnetization decay curves sampled using multiecho sequences. Some used small echo intervals (<5 ms), in *in vitro* studies, in some cases allowing semisolid protons in very short T_2 compartments to be well characterized; others used longer echo intervals ($\geq$10 ms) in imaging studies. All found a T_2-component ($T_2 = 5$–50 ms) which has been attributed to water trapped in myelin, which is generally large (about 10 %) in white matter, and which decreases in grey matter and MS lesions (see also Figure 4.3).

4.3 BIOLOGICAL BASIS OF PROTON DENSITY

In the brain, where most mobile protons (i.e. those with a T_2 long enough to be visible with MRI) are in water, PD is approximately the same as the water content of the tissue. Thus it increases with inflammation and oedema. Increases in water content have been reported in several diseases (see Section 4.6). Although PD probably correlates strongly with T_1 [see Section 4.4.1.5 and Equation (4.4)] and thus may not add much discriminating power, it does have the advantage that its biological interpretation is unambiguous and specific. In contrast, the parameters T_1 and T_2, although sensitive, produce changes that are harder to interpret.

4.4 MEASURING PROTON DENSITY – PRACTICAL DETAILS

Proton density has been estimated by a variety of methods, which are reviewed here. The MR methods differ from each other in how much they take account of short-T_2 proton water components, in how well they take account of RF nonuniformity, and whether the temperature of the external water standard, if used, has been taken account of. Receive RF nonuniformity is at its most disruptive for PD measurements, compared with other MR parameters (e.g. T_1 or T_2), where a ratio of signal intensities is used, and the effect is removed. The problems are very similar to those encountered in quantitative spectroscopy (Chapter 9), where the concentration of protons in other (nonaqueous) molecules is being estimated.

4.4.1 Published Methods for PD

4.4.1.1 Early Work

The first work consisted of collecting images with several echo times (to measure T_2 and then correct for T_2 losses) and usually at several repetition (or inversion) times (to measure T_1 and then correct for it, e.g. Bakker *et al.*, 1984; Wehrli *et al.*, 1985).

RF nonuniformity was generally ignored (although it was sometimes less of a problem, with low static fields, body coil excitation and larger head coils).

Although a linear relationship between PD and signal has been demonstrated using test objects with different values of PD (obtained by mixing water with varying amounts of D_2O; Lerski *et al*., 1984; Farace *et al*., 1997), this approach to 'calibration' takes no account of T_2 or T_2^* losses, of RF nonuniformity or of coil loading (all of which are likely to be different in the test object and the subject; Brix *et al*., 1990).

Brix *et al*. (1990) measured proton fractions in various tissues taken from rabbits, motivated by the desire to measure absolute hydrogen density for neutron therapy planning. He looked at multiecho data down to $TE = 2$ ms, and examined FIDs collected with a sampling time of 9 μs. A correction for RF nonuniformity was made using a cylindrical aqueous test object, although he recognized that nonuniformity in a subject might be different. He found large proton fractions with $T_2 <$ 10 ms (i.e. too short to be imaged; see Table 4.3). Thus to talk of measuring 'proton density' from MRI is misleading, since many protons are MRI-invisible. The visible protons are thought to be the same as the water protons (see Section 4.2), and a more correct term would be 'water proton density' (wPD).

Farace *et al*. (1997) used the body coil for excitation, and a uniformity phantom to make an approximate correction for image intensity nonuniformity. The phantom was 33 cm in diameter, filled with water, and at 1 T there would be some dielectric resonance (see Chapter 2). Gradient echo sequences with $TE = 6$, 10, 14 and 18 ms ($TR =$ 1.5 s, FA = 18°) allowed correction for T_2 losses. PD values are given in Table 4.1.

Some spectroscopic measurements of brain water content (e.g. Christiansen *et al*., 1994) have been omitted from Table 4.1, as the volume of interest was a mixture of white and grey matter.

4.4.1.2 Methods that Take Account of RF Nonuniformity Using a Field Map

In principle the transmit nonuniformity can be taken account of by collecting an RF (B_1) field map, which shows the tip angle at every point in the subject. The signal from a nonideal slice profile can be calculated, for a given B_1 and T_1. The receive nonuniformity can be calculated from the B_1 field map, using the reciprocity theorem,[10] with absolute gain measured using a concentration standard. This ideal has been achieved in the brain by very few, if any, groups; it is summarized in the box on p. 000.

In a rat ischaemia model (Venkatesan *et al*., 2000), absolute water content was estimated, using a water concentrating standard, and taking account of coil RF nonuniformity, slice profile and temperature. RF nonuniformity originating from the (small) subject was negligible. The correlation between PD and directly measured water content, over a range of 79–85 pu, was $r = 0.8$, with an rms scatter of about 2 pu.

PD has been measured in trabecular bone, taking full account of RF nonuniformity, by Fernandez-Seara *et al*. (2001). The effects of transmit nonuniformity ('excitation profile'), slice profile and receive nonuniformity were all taken account of (Figure 4.4). Flip angle maps were created[11] using the ratio of signals from two spin echoes, with nominal excitation pulses 45 and 90°. They appeared to ignore the effect of temperature on the concentration standard, and phase shifts within the slice profile were not explicitly treated. Slice profiles of the 45 and 90° sequences used for field mapping were similar, and no explicit correction was made. Failure of the reciprocity theorem at high field was discussed. Five almost-relaxed spin echo images ($TR = 4$ s) were acquired: two with short TE (16 ms), and nominal flip angles of 45–180 and 90–180°, respectively; then three with increasing TEs (24, 40 and 56 ms) and nominal flip angles 90–180°. The increasing echo times were provided using a fast spin echo sequence (RARE, echo train length 8), with T_2 magnetization preparation. From the first two, the B_1 map

[10] These concepts in RF nonuniformity are discussed more fully in Chapter 2.

[11] Two spin echo images, the first with excitation pulses θ, 2θ and the second with $\theta/2$, 2θ, were collected. The nominal value of θ was 90°. The ratio of the first to the second signal is $(\sin\theta)/[\sin(\theta/2)] = 2\cos(\theta/2)$.

Table 4.3. Proton compartments thought to be in myelin water

Source of tissue	Reference	Echo interval	Tissue type	Size[a] (%)	T_2 (ms)
Rabbit brain[b]	Brix *et al.* (1990)	2 ms	White matter	5	4
			Grey matter	Absent	
Pathological tissue from brain autopsy	Fischer *et al.* (1990)	2.3 ms	White matter	10	12
			Grey matter	4	11
Cat brain[c]	Menon *et al.* (1992)	0.4 ms	White matter	7	13
			Grey matter	Absent	
Crayfish[d]	Menon *et al.* (1992)	1.6 ms	Abdominal nerve cord	7	50
Guinea-pig[e]	Stewart *et al.* (1993)	0.4 ms	Spinal cord	13	10
Toad[f]	Does and Snyder (1995)	1.6 ms	Peripheral nerve	16	16
Human *in vivo* brain[g]	Vavasour *et al.* (1998)	10 ms	White matter	10.6	10–50
			Grey matter	3.1	10–50
			MS lesions	4.6	10–50
Garfish[h]	Beaulieu *et al.* (1998)	1.6 ms	Olfactory U	Absent	
			Trigeminal M	14	34
			Optic M	16	49
Bovine[i]	Stanisz *et al.* (1999)	2.0 ms	Optic nerve	32	22

[a] Fraction of protons in this compartment.
[b] The FID was examined with a sampling time of 9 μs; large solid compartments with $T_2 < 2$ ms were seen (white matter, 25 %; grey matter, 16 %). The assignment of the $TE = 4$ ms component in white matter to intramyelin water is speculative.
[c] Freshly excised ($n = 6$).
[d] A small pool with shorter T_2 was also seen (2 % with $T_2 = 7$ ms).
[e] Brain data could not properly distinguish grey and white matter. A solid signal, decaying in 20–200 μs, was seen.
[f] The T_2 component at 16 ms was also seen, with imaging, in the nerve, but not in muscle.
[g] From 10 normals and nine MS patients. Standard errors in the compartment size are 0.3–0.7 %. These confirm earlier measurements from the same group (MacKay *et al.*, 1994; Whittall *et al.*, 1997).
[h] The olfactory nerve is unmyelinated (U); the trigeminal and optic nerves are myelinated (M). A small component with shorter T_2 was also seen in all three tissues (3–6 %, $T_2 = 8$–17 ms).
[i] See also Chapter 8 (Figure 8.6a). The pool with $T_2 = 22$ ms is in close magnetization transfer contact with a pool of bound protons ($T_2 = 9$ μs), presumably in lipid.

was calculated; from the last four, the signal amplitude at $TE = 0$ was estimated (using an exponential fit for signal vs TE).

4.4.1.3 Myelin Water Estimation by Multiecho Acquisition

MacKay *et al.* (1994) and Whittall *et al.* (1997) have used multiecho acquisition to identify groups of water protons with distinct T_2 values. They identify three water compartments in the T_2 spectrum: a minor peak with $T_2 = 10$–50 ms, assigned to water trapped between myelin bilayers; a major peak with $T_2 = 70$ ms assigned to intra- and extracellular water, and a small peak with $T_2 >$ 1 s assigned to CSF. A single 10 mm slice was scanned, with $TR = 3$ s, four averages, and 25 min acquisition time. A selective 90° pulse, followed by hard (nonselective, rectangular) 180° pulses, produced 32 echoes at intervals of 10 ms. The multiecho sequence performed well, as shown by the T_2 estimates being independent of echo interval

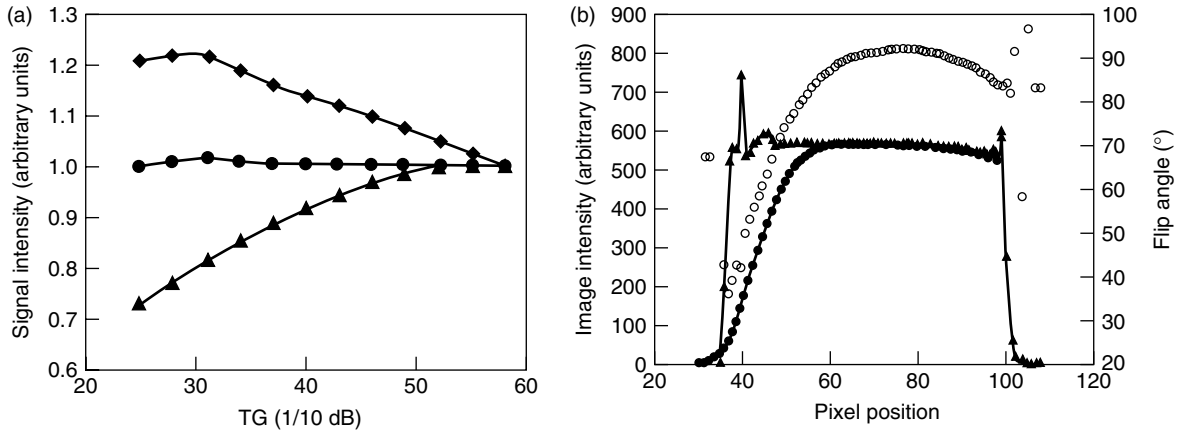

Q1 **Figure 4.4.** •(a) Normalized signal intensity before and after correction for flip angle variations. (▲) = original; (♦) = correction without taking into account slice profile; (●) = correction for flip angle and slice profile. With full correction, the signal is constant within about 3 % as transmitter output (TG) is varied by about 3.5 dB. (b) Signal intensity along a uniform phantom, towards the end of the coil (left-hand side of figure). (♦) = uncorrected signal; (▲) = signal after RF inhomogeneity correction for both flip angle and slice profile; (○) = excitation flip angle. Although both the uncorrected signal and the flip angle drop off dramatically towards the end of the coil (i.e. going towards left-hand side of figure), the corrected signal (triangles) is almost independent of distance along the coil axis. Reproduced from Fernandez-Seara, M.A., Song, H.K. and Wehrli, F.W. 2001, Trabecular bone volume fraction mapping by low-resolution MRI, in *Magn. Reson. Med.*, Copyright 2001. This material is used by permission of Wiley-Liss Inc., a subsidiary of John Wiley & Sons Inc.

(for echo spacing $TE = 10$–46 ms). (If there were significant losses through poor refocusing 180° pulses, the estimate of T_2 would decrease as the echo interval was decreased.) RF uniformity with the birdcage head coil at 1.5 T was found to be good in an oil phantom (<0.5 %) and therefore no correction was thought necessary (although the uniformity in the head might have been worse – see Chapter 2). A small correction for T_1 losses was made. A water sample in the field of view was used to establish absolute water concentrations (although no temperature correction was made). Myelin water fraction was estimated as the fraction of the total signal with T_2 values between 10 and 50 ms.

4.4.1.4 Distant Dipolar Field Method

Recently a method for measuring PD using distant dipolar field (DDF) effects has been published (Gutteridge *et al.*, 2002). A special sequence generates a small signal proportional to the square of the equilibrium magnetization, i.e. PD^2. By collecting a conventional signal, proportional to PD, and dividing, a pure PD map is obtained. RF nonuniformity effects in both the flip angle and the receive sensitivity are removed. The sequence used a pulse interval of 5 ms, and the resulting PD estimate is thought to include myelin water but not the semisolid protons.[12] A three-dimensional sequence was used, with $TR = 12$ s and eight averages, giving a $64 \times 64 \times 8$ matrix in 13 min. The spatial resolution of results presented at 3 T is relatively poor [$3 \times 3 \times 7$ mm; see Figure 4.2 (Plate 2)]. It may be possible to use this methodology, combined with a conventionally acquired, high-resolution, PD map to remove the effects of RF nonuniformity (which vary slowly with position) from the latter. The results are presented as values for M_0, the equilibrium magnetization, with normal white matter having $M_0 = 6.5 \times 10^{-3}$ A m^{-1}. Water (at room temperature, 18 °C) has $M_0 =$

[12] Private communication from R. Bowtell.

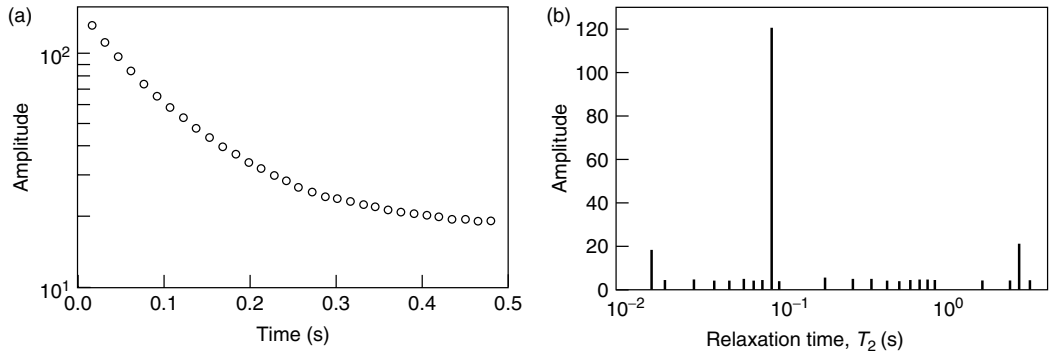

Q1 **Figure 4.5.** •(a) Decay of transverse magnetization in normal-appearing white matter (1.8 ml volume of interest). The echo interval is 15 ms [later work (Whittall *et al.*, 1997) used 10 ms). (b) T_2 relaxation distribution from the decay curve shown in (a). Three components of water protons are assigned to: (i) water trapped between layers of myelin ($T_2 = 10–55$ ms); (ii) water in cytoplasmic and extracellular spaces ($T_2 = 70–95$ ms); (iii) CSF ($T_2 > 1$ s). Reproduced from MacKay, A., Whittall, K., Adler, J., Li, D., Paty, D. and Graeb, D. 1994, In vivo visualization of myelin water in brain by magnetic resonance, in *Magn. Reson. Med.*, Copyright 1994. This material is used by permission of Wiley-Liss Inc., a subsidiary of John Wiley & Sons Inc.

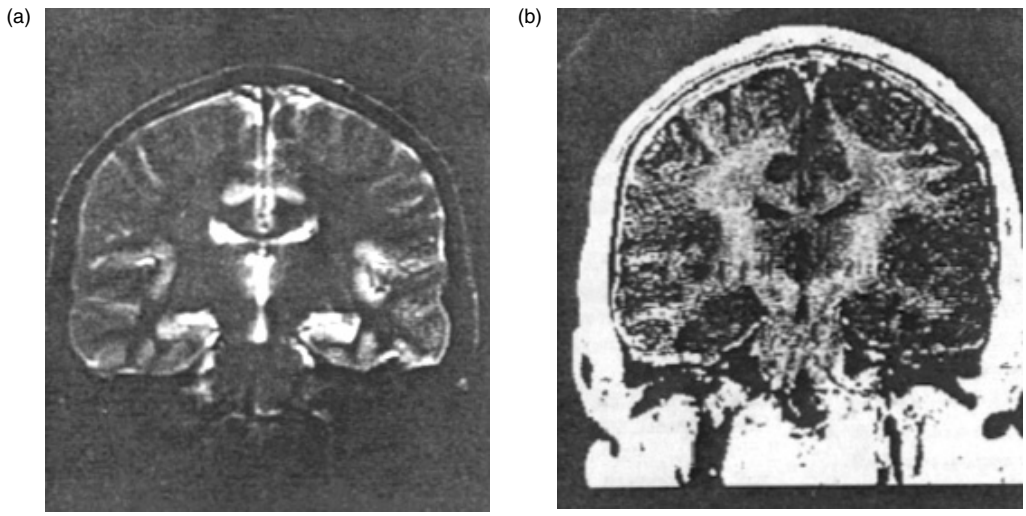

Q1 **Figure 4.6.** •(a) Coronal image ($TE = 60$ ms) of a normal volunteer, using 32-echo sequence. (b) Corresponding image of short-T_2 fraction, indicative of myelin. Reproduced from MacKay, A., Whittall, K., Adler, J., Li, D., Paty, D. and Graeb, D. 1994, In vivo visualization of myelin water in brain by magnetic resonance, in *Magn. Reson. Med.*, Copyright 1994. This material is used by permission of Wiley-Liss Inc,, a subsidiary of John Wiley & Sons Inc.

9.92×10^{-3} A m^{-1}; at body temperature (310 K), this is reduced[13] to 9.31×10^{-3} A m^{-1}, and this is used to calculated PD values (Table 4.1).

[13] Not 9.4 as stated in the paper (private communication from R. Bowtell). The change in water density with temperature was ignored.

4.4.1.5 Estimation of Water Content from T_1

Water content and T_1 value correlate closely in some studies, and it is possible to estimate water content quite accurately from measured *in vivo* T_1 values (Fatouros and Marmarou, 1999). A model for the observed T_1, based on the contribution

from bound water, predicts its field dependence (Fatouros *et al*., 1991). Mackay and Whittall argue that this bound water is the myelin water measured in their multiecho method (Whittall *et al*., 1997). At 1.5 T the relationship is (Fatouros and Marmarou, 1999):

$$100 \text{ pu/water content} = 0.921 + 0.341 \text{ s}/T_1 \quad (4.4)$$

The reported T_1 of bulk water at 37 °C was 4.35 s [this gives a water content of 99.9 pu in Equation (4.4)]. A water content of 71 pu (the value for white matter) implies a T_1 of 700 ms, which is realistic. A comparison (Fatouros and Marmarou, 1999) of gravimetrically determined water content values with MRI-derived values [from T_1 using Equation (4.4)], in 11 biopsy samples from eight subjects with brain tumours, showed good correlation ($r^2 = 0.976$), with a mean absolute error of 0.7 pu (Figure 4.7).

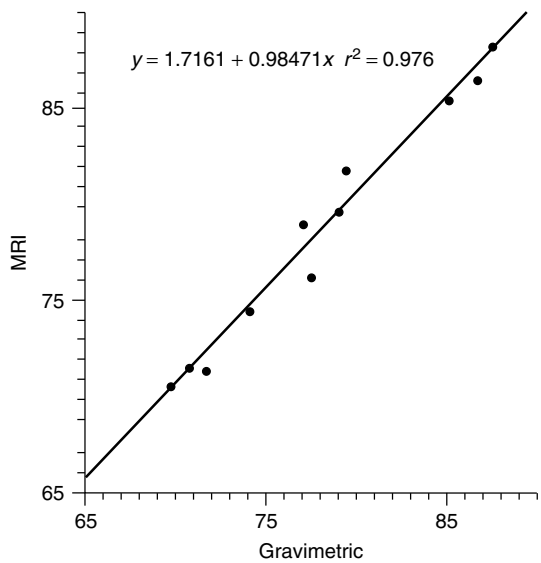

Figure 4.7. The high correlation between water content estimated from MRI T_1 value [from Equation (4.4)] and water content determined gravimetrically, for a range of tumour biopsy samples. Reproduced from Fatouros, P.P. and Marmarou, A. 1999, Use of magnetic resonance imaging for *in vivo* measurements of water content in human brain: method and normal values, in *J. Neurosurg.*, Copyright 1999 Institute of Neurology

Venkatesan *et al*. (2000) also found a strong relationship ($r = 0.93$) between water content and T_1 in a rat cerebral ischaemia model, over a range of water content values 79–85 %, although the coefficients in their equation are quite different from those in Equation (4.4) (100 pu/water content $= 0.01 + 3.0$ s/T_1).

These strong relationships would not necessarily hold in other pathologies; nonetheless, it implies that PD and T_1 information may be very correlated, and that when it comes to discriminating tissues using multiple MR parameters there may be little value in measuring both PD and T_1.

4.4.2 Principles of Measuring PD

4.4.2.1 Concentration Standards for PD

A range of test objects with differing PD can be made by using varying concentrations of deuterium oxide (D_2O) in water (Lerski *et al*., 1984; Gutteridge *et al*., 2002). However the cost may be prohibitive for large objects, and an alternative is to use agarose gel loaded with small glass beads (0.1 mm diameter; Waiter and Lerski, 1991), although there is a possibility that susceptibility effects might reduce T_2^* to an unacceptably low value for EPI.

If the signal is known to increase linearly with PD (as is usually the case, unless the receiver gain is being altered in order to keep within a particular dynamic range), then a single concentration standard will usually suffice. Water (doped to reduce its T_1 value) is the obvious choice.

Temperature dependence of signal. The signal from such test objects or standards at room temperature differs from the same object at body temperature (see Figure 4.8) for two reasons: first the magnetization M_0 of a given number of protons is inversely proportional to absolute temperature. This corresponds to a reduction of 0.34 %/ °C at 20 °C, and 0.32 %/ °C at 37 °C. Thus the signal at room temperature (about 20 °C) will be approximately 5.5 % higher than at body temperature (37 °C). This was confirmed by phantom measurements of effective spin density vs temperature, over the range 17–36 °C, which did indeed show a decrease of 0.32 %/ °C (Venkatesan *et al*., 2000).

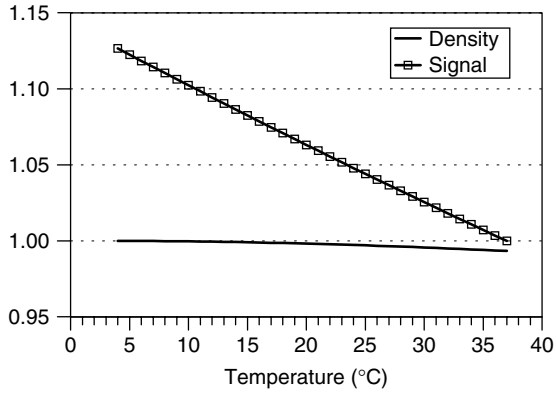

Figure 4.8. The dependence of water signal on temperature. A small factor arises from the decrease in density; a much larger factor arises from the decrease in magnetization with temperature (proportional to the inverse absolute temperature); see Table 4.4 and Section 4.4.2

Second, the density of water at room temperature is about 0.5 % higher than at body temperature; this small increase in the number of protons will increase the signal at room temperature by this amount. The signal from the standard, S_{Ts}, measured at a temperature T_{s} °C, should be converted to the equivalent value (S_{37}) that it would have at body temperature (37.0 °C = 310.2 K):

$$S_{37} = S_{\mathrm{Ts}} \frac{\rho_{37}}{\rho_{\mathrm{Ts}}} \frac{273.2 + T_{\mathrm{s}}}{310.2} \qquad (4.5)$$

Density values are given in Table 4.4, and conversion factors for signal measured from a standard at a range of temperatures are given. If the phantom has been kept refrigerated[14] before being imaged, the correction factor will be even larger (up to 11 %). Thus for high accuracy the phantom temperature should be recorded, and the signal from the standard corrected to obtain the body temperature value.

If a large-diameter concentration standard is used, as part of a scheme to estimate the RF nonuniformity, then this must be based on a nonaqueous liquid, such as oil (to avoid RF standing wave effects; see Chapter 3), and the temperature dependence of its density must be found.

[14] A typical refrigerator temperature is 5 °C.

Table 4.4. Temperature correction factors for water concentration standard

Temperature of concentration standard, T_{s} (°C)	Density of water[a] (kg m^{-3} × 10^3)	S_{37}/S^b_{Ts}
4	1.0000	0.8877
5	1.0000	0.8909
6	1.0000	0.8941
7	0.9999	0.8973
8	0.9999	0.9006
9	0.9998	0.9039
10	0.9997	0.9071
11	0.9996	0.9104
12	0.9995	0.9137
13	0.9994	0.9170
14	0.9993	0.9204
15	0.9991	0.9237
16	0.9990	0.9271
17	0.9988	0.9304
18	0.9986	0.9338
19	0.9984	0.9372
20	0.9982	0.9406
21	0.9980	0.9440
22	0.9978	0.9474
23	0.9976	0.9508
24	0.9973	0.9543
25	0.9971	0.9577
. . . . .		
37	0.9934	1.0000

[a] Values at 1 atmosphere, from Kaye and Laby (1959), interpolated to 1 °C intervals.
[b] Multiply the signal from the concentration standard by this factor to obtain what the signal would be at body temperature 37.0 °C (310.2 K) [see Equation (4.5)].

4.4.2.2 Existing Sequences

The existing, published sequences (principally those of Farace *et al.*, 1977; see Section 2.4.1) all suffer from poor coverage and generally have too much T_1-weighting (i.e. too short a *TR*) for the brain. The DDF method requires a special sequence, and its SNR is too low for general use.

Whatever the sequence, the image datasets should be spatially registered if possible. Ideally a concentration standard should be measured (see Section 4.4.2.1 and the box on p. 000). The experience from spectroscopy suggests that collecting

a separate dataset from the standard, located at the coil centre, is the best procedure, rather than using a standard attached to the side of the head, or an internal reference tissue. Provided the scanner gain is controlled, this signal is stable over long time periods (until the next scanner upgrade).

After considering general principles in the next three sections, several new approaches will be proposed.

4.4.2.3 T_2*-weighting*

T_2 losses cannot be avoided by using a single short echo time. At $TE = 10$ ms, assuming monoexponential behaviour, then $T_2 = 90$ ms and there is 11 % signal loss. The myelin water, with $T_2 = 10-50$ ms, will suffer even more loss. Multiple spin echoes have been used by Mackay and Whittall, as part of a scheme to determine myelin water. However this approach has poor coverage, and there is significant T_1-weighting ($TR = 3$ s). Extension to multiple slices is unlikely, given the problems of slice refocusing, SAR and MT effects (Vavasour *et al*., 1998).

Multiple gradient echoes, as used by Farace, hold more promise, since they can be used at shorter *TR* without incurring T_1 losses (by using a reduced flip angle). A map of T_2^* is produced as a by-product, which may be useful in some situations, and may relate quite strongly to the T_2 of the myelin water.

Given the presence of at least two T_2 components, the particular details of which *TE*s are used, and how the T_2 correction is made, will have some influence on the signal value extrapolated back to $TE = 0$.

4.4.2.4 T_1*-weighting*

If lesions with increased T_1 are to be accurately measured, sequences with minimal T_1 losses are required. In principle, tissue with T_1 values up to that of CSF may exist. The T_1 of CSF is independent of field strength, and is about 3.5–4.0 s (Clare and Jezzard, 2001) at body temperature.[15] In MS, lesion values up to 2 s (at 1.5 T) are seen (Stevenson *et al*., 2000). The simplest approach is to use sequences that have acceptable T_1 losses up to this value. Figure 4.9 shows the signal losses arising from long T_1 values, and can be used as a design aid in choosing an appropriate flip angle for a gradient echo sequence with a given *TR*.

An alternative, more complex approach is to allow the PD-weighted sequences to have more T_1-weighting (up to perhaps 10 % losses). The flip angle is increased, giving a higher SNR. A T_1-weighted sequence is also collected. T_1 can then be measured, for example using the dual flip angle method, with correction for RF nonuniformity and slice profile, following the method of Parker *et al*. (2001). The T_1 value is then used to correct the PD-weighted images. The benefit of this approach is that the signal in the PD-weighted images is increased, and a more efficient use of the scanning time can be made. The T_1 values may also be useful in their own right. A potential problem is that, in voxels containing a small amount of CSF, the resulting multiexponential recovery may not be properly characterized by a simple T_1 measurement, and the relaxed CSF signal may not be accurately estimated.

4.4.2.5 RF Nonuniformity

4.4.2.5.1 Simple Approach Without a Field Map

The intrinsic uniformity of the RF coil, and of the field inside the head, may be so good that no correction is necessary. An internal concentration standard, such as contralateral tissue, may be acceptable. The symmetry of the coil can be tested by looking at controls. The coil uniformity can be investigated using a uniform phantom. The effect of the head itself depends on frequency and hence the value of B_0; even at 1.5 T the nonuniformity seems to be significant (see Chapter 2).

If the nonuniformity in the head is thought to be close to that in a uniform standard (i.e. if the effect of the head itself is small), then a uniform phantom can be used as a concentration standard, and absolute values of PD obtained. Proper note must be taken of the phantom temperature and the transmitter voltage used during the pre-scan

[15] Allen *et al*. (1986) measured CSF at 2.4 T, finding $T_1 = 3.9 + 0.1$ s, $T_2 = 2.5 + 0.1$ s.

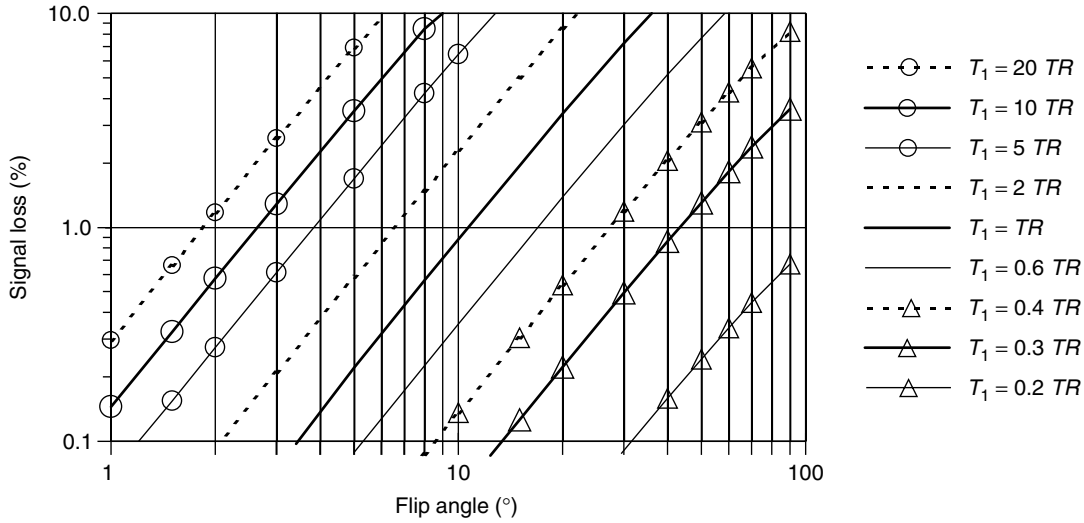

Figure 4.9. T_1-losses in a gradient echo or spin echo sequence. For a PD sequence, a combination of TR and FA can be chosen to give T_1-losses less than a prescribed amount, for particular tissues. Thus normal white matter ($T_1 = 600$ ms), imaged with a sequence with $TR = 1000$ ms (i.e. $T_1 = 0.6\ TR$), needs a FA of no more than 17° for the T_1 losses not to exceed 1 %. At this TR and FA, a lesion with $T_1 = 2$ s would suffer 6 % signal loss. The signal losses were calculated using the equation $S = S_0[1 - \exp(-TR/T_1)]\sin(\theta)/[1 - \cos(\theta)\exp(-TR/T_1)]$; the fully relaxed signal is $S_0 \sin(\theta)$, and the fractional signal loss is $[1 - \cos(\theta)]\exp(-TR/T_1)/[1 - \cos(\theta)\exp(-TR/T_1)]$. At low FA and short TR, the loss is 0.015 ($FA^2 T_1/TR$) per cent (with FA in degrees), e.g. for $TR = 100$ ms, $T_1 = 2$ s, FA = 1° it is 0.3 %

procedure when the flip angle is being adjusted (see the box on p. 000).

4.4.2.5.2 Collecting a Field Map

The most accurate, thorough, time-consuming and complex approach is to collect a complete RF field map of the head. It may be acceptable to do this once only, in an average head (or at least in a small sample of heads), and reduced spatial resolution is probably acceptable (since the B_1 field will not vary rapidly with position). This information then allows complete correction for both transmit and receive nonuniformity, using the reciprocity principle (Hoult and Richards, 1976; Hoult 2000; and see Chapter 2). There are several ways of collecting a field map, depending on the dynamic range required (see Chapter 2); a simple method is the (45, 90) method used by Fernandez-Seara *et al*. (2001). A RARE version is fast, since multiple phase encodes are achieved in a single TR (see Table 4.5). Selective pulses were used, with no correction for slice profile differences, which were small.

4.4.2.6 Changes in Slice Profile

Changes in slice profile must also be considered. These occur wherever the flip angle changes (unless it is very small, and the Bloch equations are operating in the linear portion, where $\sin\theta = \theta$). Three-dimensional gradient echo sequences using hard (nonselective) pulses need no correction; however they often use broadly selective pulses to excite a slab; if so, the drop off at the edges of the slab must be taken into account. In spectroscopic imaging, the nonuniform excitation profile has been corrected to provide better quantification of metabolite concentrations (McLean *et al*., 2001). The importance of correcting for slice profile as well as FA nonuniformity is demonstrated in Figure 4.4.

The transverse magnetization, calculated from a Bloch simulation using the selective pulse shape,

Table 4.5. Published and proposed sequences for measuring PD

Sequence	*TR*	FA	*TE* (ms)	Time for whole brain ($256 \times 128 \times 28$)	References
Multiecho spin echo[a] (single slice)	3 s	90°	10–320	25 min (one slice)	MacKay *et al*. (1994), Whittall *et al*. (1997)
Four spin echoes	4 s	90°	16, 24, 40, 56	5 min[e]	Fernandez-Seara *et al*. (2001)
Four gradient echoes	1.5 s	18°	6, 10, 14, 18	13 min	Farace *et al*. (1997)
Relaxed two-dimensional gradient echoes[b]	1.0 s	6°	5, 10, 15, 20	9 min	Proposed
Relaxed three-dimensional gradient echoes[c]	100 ms	2°	5, 10, 15, 20	27 min	Proposed
Relaxed RARE field map[d]	20 s	45°, 90°	20	11 min	Adapted from Fernandez-Seara *et al*. (2001)

[a] Four averages, one single 10 mm slice.
[b] FA chosen to give <1 % loss for $T_1 = 2$ s (see Figure 4.9).
[c] This can be speeded up (e.g. $TR = 50$ ms, FA = 1.1°, total time = 14 min) if SNR will allow.
[d] *TR* has been extended to allow CSF ($T_1 = 4$ s) to fully relax. RARE sequence, ETL = 8, with excitation pulses nominally 45 and 90°, refocusing pulses nominally 180°. No slice profile correction for the selective field mapping pulses. Other schemes may be feasible (see Chapter 2).
[e] For fast spin echo (RARE) sequence, echo train length ETL = 8, five acquisitions (four *TE*s and field map), three slices, each 128×128.

is integrated over the slice profile to obtain an effective slice width for the nominal flip angle. If the sequence is not full relaxed, T_1 must be taken into account. Further details are given in Chapters 2 and 5, and by Parker *et al*. (2001).

4.4.3 Protocols for Measuring PD

Existing protocols, and proposed two- and three-dimensional gradient echo sequences, are shown in Table 4.5. The proposed sequences, combined with field mapping, do appear feasible, although they have not been tried. The principles of using field mapping to measure PD are summarized in the box on p. 000, with simplifications to allow the use of a uniform test object in place of explicit field mapping.

Measuring PD in an arbitrary nonuniform RF field:[16] reciprocity to the rescue

(1) Measure an RF field map $B_1(\mathbf{r})$[17]• for a given transmitter output. Reference this to standard position ($r = 0$), usually the coil centre, to obtain the tip angle at $r = 0$ [i.e. $\theta(0)$], and a relative field map $b_1(\mathbf{r})$:

$$b_1(\mathbf{r}) = B_1(\mathbf{r})/B_1(0) \qquad (4.B.1)$$

[16] See also Fernandez-Seara *et al*. (2001) for a similar scheme.

[17] Ideally in the head, but it may be acceptable to do this is a uniform test object (see Chapter 3). This scheme assumes the same head coil is used for both transmission and reception. Using a body coil for transmission gives little benefit for PD mapping, since the receive (head coil) nonuniformity must be characterized – See Chapter 12.

The tip angle at any location is then

$$\theta(\mathbf{r}) = b_1(\mathbf{r})\,\theta(0) \qquad (4.B.1)$$

(2) Measure the relaxed signal at several echo times, fit an exponential model, and derive the signal S at $TE = 0$.[18]

(3) The signal from a relaxed gradient echo is

$$S(\mathbf{r}) = g(\mathbf{r})\frac{T_0}{T}\frac{\rho_T}{\rho_0}\mathrm{PD}(\mathbf{r})\,SW[\theta(\mathbf{r})]\sin\vartheta(\mathbf{r}) \qquad (4.B.3)$$

where $g(\mathbf{r})$ is the gain at position $\mathbf{r}$ (i.e. the signal when a 90° pulse is applied to a sample with unit PD at the reference temperature, T_0). $SW[\theta(\mathbf{r})]$ is the effective slice width, calculated from the integral of the slice profile, which depends only on the local flip angle at the slice centre, $\theta(\mathbf{r})$.[19] T is the absolute temperature (temperature in $^\circ\mathrm{C} + 273$), and T_0 is a reference temperature (usually body temperature is a convenient choice). Sin θ is the response function[20] for a gradient echo. ρ_0 and ρ_T are the densities of water at T_0 and T respectively. The T and ρ terms describe how the magnetization, M_0, depends on the absolute temperature and the density [see Section 4.4.2.1 and Equation (4.5)].

(4) The reciprocity theorem[21] states that $g(\mathbf{r})$ is proportional to the flip angle $\theta(\mathbf{r})$ at the same location, for a fixed transmitter output. Also $\theta(\mathbf{r})$ is proportional to the transmitter output voltage V.[22] Thus

$$g(\mathbf{r}) = \alpha\theta(\mathbf{r})\frac{V_0}{V} \qquad (4.B.4)$$

where V_0 is any convenient standard transmitter voltage, and α is a constant that depends only on the RF coil. The signal is then [from Equations (4.B.2)–(4.B.4)][22]

$$S(\mathbf{r}) = \alpha b_1(\mathbf{r})\theta(0)\frac{V_0}{V}\frac{T_0}{T}\frac{\rho_T}{\rho_0}\mathrm{PD}(\mathbf{r})SW \times [b_1(\mathbf{r})\vartheta(0)]\sin[b_1(\mathbf{r})\vartheta(0)] \qquad (4.B.5)$$

(5) The only unknown (apart from PD) is α, which relates the gain to the tip angle. This is determined by measuring the signal[23] from a water concentration standard, with proton density PD^s and ordinary density ρ_s at its temperature T_s, located at the reference location ($\mathbf{r} = 0$)

$$S^s = \alpha\theta^s(0)\frac{V_0}{V_s}\frac{T_0}{T_s}\frac{\rho_{Ts}}{\rho_0}\mathrm{PD}^s SW[\vartheta^s(0)] \times \sin[\vartheta^s(0)] \qquad (4.B.6)$$

During this measurement the transmitter voltage is V_s and the tip angle at the reference position is $\theta^s(0)$. Either $\theta^s(0)$ is set by the autopre-scan procedure to a known value (such as 90°), by adjusting V_s, or V_s can be left unchanged and $\theta^s(0)$ determined by the field mapping technique. The receiver gain is best left unchanged; if it is altered, a correction to the signal can be made, provided the size of the change is accurately known.

[18] Also make T_1 corrections if needed.

[19] The transverse magnetization, calculated from a Bloch simulation using the selective pulse shape, is integrated over the slice profile to obtain an effective slice width for the nominal flip angle $\theta(\mathbf{r})$. If the sequence is not full relaxed, T_1 must be taken into account (see Chapter 2). For a three-dimensional sequence, the slice profile effects can usually be ignored ($SW = 1$), unless a broadly selective pulse has been used, in which case its excitation function must be included (McLean *et al*., 2001).

[20] For a spin echo the response function is $\sin^3\theta$ (Fernandez-Seara *et al*. 2001).

[21] See Chapter 2.

[22] By monitoring the transmitter output voltage required to achieve a give FA, differences in sample loading of the coil are taken into account. On a General Electric scanner, V proportional to $10^{\mathrm{TG}/200}$, where TG is the 'transmitter gain' in units of 0.1 db.

[23] If the signal is collected over an extended area, it may be necessary to take account of nonuniformity in that area by integration. Near the centre of the coil this should not be necessary.

(6) The PD map for brain is then obtained from box Equations (4.B.5) and (4.B.6):

$$\mathrm{PD}(\mathbf{r}) = \frac{S(\mathbf{r})}{S_s b_1(\mathbf{r})}\mathrm{PD}^s \frac{\vartheta^s(0)}{\vartheta(0)}\frac{V}{V_s}\frac{T_{37}}{T_s}\frac{\rho_{Ts}}{\rho_{37}} \times \frac{SW(0)}{SW(\mathbf{r})}\frac{\sin[\vartheta^s(0)]}{\sin[b_1(\mathbf{r})\vartheta(0)]} \quad (4.B.7)$$

where S, b_1, $\theta(0)$ and V are the values measured for the brain at the time of scanning. ρ_{37} is the density of water at brain temperature (T_{37} K). The factor $(T_{37}\rho_{Ts})/(T_s\rho_{37})$ is the inverse of the factor tabulated in Table 4.4.

(7) A simpler scheme, which does not involve collecting a field map, and instead uses a large uniform standard, is possible. The major assumption is that the nonuniformity of the RF field is the same in the standard as in the head. Provided the field is not too high (1.5 T may be acceptable) and that the standard contains oil and not water, this is a reasonable working assumption (see also Chapter 3).

The signal from the uniform standard is [from Equation (4.B.5)]:

$$S^s(\mathbf{r}) = \alpha b_1^s(\mathbf{r})\theta^s(0)\frac{V_0}{V_s}\frac{T_0}{T_s}\frac{\rho_{Ts}}{\rho_0}\mathrm{PD}^s SW \times [b_1^s(\mathbf{r})\vartheta^s(0)]\sin[b_1^s(\mathbf{r})\vartheta^s(0)] \quad (4.B.8)$$

where $b_1^s(\mathbf{r})$ is the nonuniformity in the standard. Provided the standard and the head have the same nonuniformity $b_1(\mathbf{r})$ and FA at the centre $\theta(0)$, then the receive, transmit and slice profile terms all cancel, and dividing Equations (4.B.5) and (4.B.7) gives:

$$\mathrm{PD}(\mathbf{r}) = \frac{S(\mathbf{r})}{S_s(\mathbf{r})}\mathrm{PD}^s\frac{V}{V_s}\frac{T_{37}}{T_s}\frac{\rho_{Ts}}{\rho_{37}} \quad (4.B.9)$$

4.5 FACTORS WHICH CAN ALTER THE MEASURED VALUE OF PD

4.5.1 Normal Biological Variation

There is probably some normal intra-subject variation in PD caused by changes in hydration status arising from alcohol intake, menstruation, various infections and drug treatments, although these have not been explicitly studied in detail.

4.5.2 Instrumental Factors

RF nonuniformity is probably the most important factor; this leads to a tip angle and a receive sensitivity that vary with position. Aqueous uniformity phantoms have large RF standing wave effects, particularly when large and at high static field, leading to a dome-shaped response (Tofts, 1994). See Chapters 2 and 3 for a detailed discussion on this, and an illustration of nonuniformity in the head at 1.5 T, even with a uniform excitation coil. In the absence of correction, the effect is usually to reduce the apparent PD at positions away from the coil centre.

If absolute PD is required, an external proton standard must be measured, and it must be possible to control the gain of the scanner in a predictable way. If the temperature of the external standard is not taken account of, PD will be underestimated by 6–11 % (see Table 4.4). CSF is sometimes used as an internal standard, but it is generally unsatisfactory, because of its long T_1, its motion in response to cardiac pulsation, and the difficulty in finding large volumes of CSF in which to measure the signal. An external standard attached to the head has been used, but experience from spectroscopy suggests these are not satisfactory. They are generally small, located in a region of high nonuniformity, have uncertain temperature, and often have an undefined position (making nonuniformity correction inaccurate).

Subject motion can degrade image datasets collected serially, and image registration is desirable to realign datasets to within a pixel.

Transmitter nonlinearity (Venkatesan *et al.*, 1998), if present, may make corrections for

nonuniform B_1 difficult. Modern scanners are unlikely to have large amounts of nonlinearity (otherwise selective pulses would not work properly, and imaging artefacts would be seen).

Magnetization transfer effects will reduce the signal of free water, even though *TR* is long, if there are too many off-resonant pulses applied. MTR theory (Chapter 8) can be used to estimate the magnitude of their effect. ASL imaging of perfusion is affected by MT effects (see Chapter 13). A practical test is to switch off the multislice imaging and observe whether the signal from a single slice had been reduced.

A summary of the factors to consider when looking at potential methods for measuring total PD is given in the Box on p. 000; the author has not found a single publication that takes account of all of these factors.

Six questions to ask when assessing published methods for measuring absolute PD

- **Have T_1 losses been considered?** A spin echo sequence needs $TR > 5\,T_1$, i.e. 20 s to handle CSF; a shorter *TR* might be acceptable, although lesion T_1 values can approach that of CSF.
- **Have T_2 losses been considered?** Even at a short *TE* of 5 ms, the signal loss is 5 % for $T_2 = 90$ ms, and more for short-T_2 myelin water. Matching with a phantom having the same T_2 as the subject does not address T_2 increases brought about by disease.
- **Have RF nonuniformity effects in the subject's head been assumed to be the same as in a phantom?** Standing wave effects in the head can be significant, even at 1.5 T, and cannot be measured by a uniform phantom.
- **Has the dependence of RF nonuniformity on T_1 been taken account of?** This can be bypassed by using a relaxed sequence, i.e. $TR \gg T_1$ for a spin echo, and a low enough flip angle for a gradient echo sequence.
- **Have changes in slice profile with position and T_1 been taken account of?** Bloch equation nonlinearities change the slice profile wherever the FA is changed, thus affecting the slice thickness.
- **Have coil loading and temperature differences between the subject and the concentration standard been taken account of?**

4.5.3 Model Factors – Multiexponential T_2 Behaviour

The proton signal will be partly attenuated by T_2 losses, depending on the minimum *TE* used, the interecho interval and T_2. Determining a monoexponential T_2 and then correcting the shortest echo time dataset with this T_2 value will partly correct the attenuation. Fitting a multiexponential model will recover the myelin water signal ($T_2 \approx$ 10–50 ms) more fully. However in the absence of full knowledge of the T_2 values and T_2 distribution for the myelin water, we must assume that the PD estimate that we obtain will be dependent, to some extent, on the minimum *TE* used, the interecho interval, and the precise method of fitting.

4.6 CLINICAL APPLICATIONS OF PROTON DENSITY

In *tumours*, PD was found to be 14–20 pu higher than normal white matter (Just and Thelen, 1988), although the values did not enable different tumour types to be distinguished, even when used in conjunction with T_1 and T_2 values. The range of measured normal values for grey matter was large (grey/white ratio = 1.16 SD = 0.07), and poor precision (reproducibility) in the measurement procedure may have contributed to this failure. A second explanation is that a high correlation between PD and T_1, as reported by Fatouros and Marmarou (1999), mean that PD did not contribute any extra information.

In stroke, water content between 4 and 7 days after the insult was increased ($p < 0.005$) compared with normal values (Gideon *et al.*, 1999).

The treatment effect of drugs to reduce *cerebral oedema* has been monitored using indirect measurement of water content. The high correlation with T_1 has already been noted (Figure 4.7). Bell *et al*. (1987) used measurements of T_1 that had been calibrated to give a good estimate of water content, to observe the short-term effects of drug treatment. In 11 patients with tumours of glial origin, dexamethasone had no effect on T_1, even though the patients improved clinically after treatment, suggesting that the mechanism of action is not that of reducing water content. In contrast, mannitol reduced the T_1 of all 11 patients, by an average of 32 ms (compared with normal T_1s in white matter of 298 ms at 0.08 T); this corresponded to an estimated mean reduction in water content of 1.42 pu within the oedematous tissue.

In multiple sclerosis, the myelin water method of Mackay and Whittall (MacKay *et al*., 1994; Whittall *et al*., 1997; see Figure 4.5 and 4.6) has been used to measure total water content (as inferred from PD) and myelin water fraction (Laule *et al*., 2002). An internal grey matter water concentration standard was used. MS lesions had 7.7 % higher water content than normal-appearing white matter (NAWM), and their myelin water fraction was reduced to half its normal value (confirming an earlier report by Vavasour *et al*., 1998). Compared with normal white matter, NAWM had 1.8 % higher water content, and 15 % lower myelin water fraction.

True water content has been shown to be raised in some diseases, using post-mortem tissue. This implies that PD is probably increased in life in these diseases, and that MRI measurements would be able to detect a change. In a case of subacute sclerosing leukoencephalitis (Norton *et al*., 1966), white matter water content was raised to 85 pu (well above the normal value of 72 pu, and exceeding that of grey matter; see Table 4.2); this was thought to be typical of severe demyelination. In multiple sclerosis (Tourtellotte and Parker, 1968), the water content of NAWM was raised (74 pu compared with a normal value of 71 pu), and lesions had very elevated water content (85 pu). In a study of 11 patients with gliobastomas (Takagi *et al*., 1981), biopsy water content was 5–8 pu greater than in normal white matter (which had water content = 70 pu). White matter adjacent to an arteriovenous malformation has greatly raised water content (85 pu). Two patients who had received mannitol (a treatment given to reduce brain water content) had water content values 5 pu below normal.

4.7 CONCLUSIONS – THE FUTURE OF PROTON DENSITY MEASUREMENTS

Proton density is a paradoxical MR parameter, the poor relation in the family of MR parameters. It underlies almost every MR measurement we make; the MR signal is proportional to it; the first MR images were essentially showing PD; yet this Chapter is necessarily short, because we have little experience of how to measure it, and even less experience of using it clinically. In the early days of MRI its small dynamic range (from about 70 to 100 pu) led to its dismissal by parameters with larger range (e.g. T_1, from about 200 ms to 4 s). Now we have greater signal-to-noise ratios, a better understanding of the importance of multiparametric measurements, and the knowledge to make absolute PD measurements, without degradation by RF nonuniformity, partly as a result of experience from spectroscopy. RF nonuniformity and gain changes affect spectroscopic measurements of the concentration of other proton-containing compounds (see Chapter 9), and it is to be expected that progress and experience in each field will benefit the other.

From the technical point of view, the optimum sequence is still to be identified; the multiple spin echo approach may be nonviable, and gradient echo approaches may be the way to obtain whole-brain coverage, although measurement of myelin water will not then be possible. For characterization of oedema this may be satisfactory. The importance of temperature in estimating absolute values of PD will become recognized. As clinical scanners move to higher field, characterizing and removing the effects of RF nonuniformity will become increasing important.

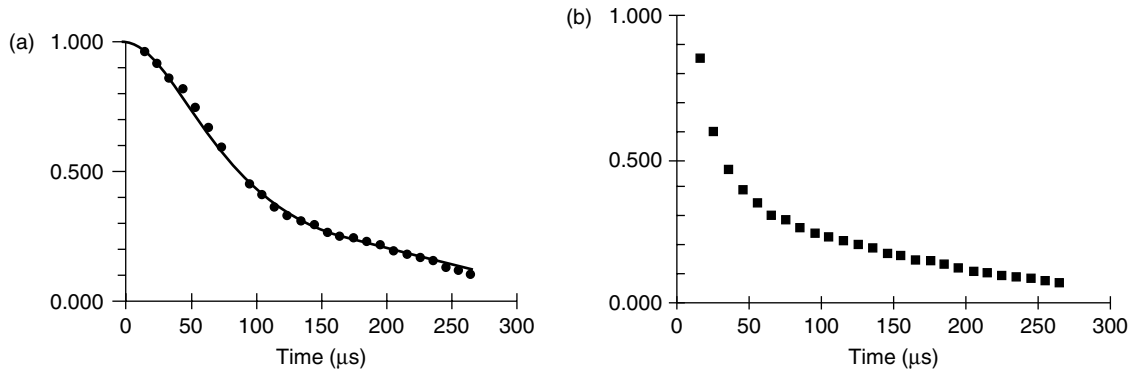

Figure 4.10. Multiecho signal from the solid proton fraction (a) in a model lipid bilayer system and (b) in a cancer cell line. Echo spacing is 10 μs. The lipid signal could be fitted to a theoretical expression. The signal from the mobile proton component has been subtracted. This is 10 % of the raw lipid signal, and 35 % of the raw cancer cell signal. Reproduced with permission from Bloom, M., Holmes, K.T., Mountford, C.E. and Williams P.G. 1986, Complete proton magnetic resonance in whole cells, in *J. Magn. Reson.*, Copyright 1986 Elsevier Science Ltd.

From the biological point of view, more studies on the water trapped in myelin are called for, particularly at shorter echo times than are currently used. What is the T_2 or range of T_2 values in myelin water. Measurements on post-mortem tissue using an echo interval of 2.3 ms (Fischer *et al.*, 1990) find $T_2 = 11–12$ ms, and suggest that *in vivo* echo intervals of 10 ms are too long to characterize these protons sufficiently well; see Table 4.3). What is their T_1? What is the optimum *TR* to use when imaging these protons? Can the coverage of the current sequences be improved? How well do myelin water measurements agree with measurements of the bound proton fraction (thought to be located largely in myelin lipid) made using quantitative MT measurements [see Chapter 8, Table 8.2 and Figure 8.6(a)].

The assignment of proton pools still requires some more direct evidence. The solid pool, although large, has been studied very little (Bloom *et al.*, 1986; Brix *et al.*, 1990; Ramani *et al.*, 2001). Systematic multiple-echo measurements on human post-mortem or biopsy tissue, at short echo times (down to 10–20 μs), looking at white matter, grey matter and MS lesions, would clarify and possibly confirm current views (see Figure 4.10). A preliminary multiecho study (Ramani *et al.*, 2001) of the solid lipid protons in fixed brain tissue showed a pool in normal white matter (12–25 % of protons, $T_2 = 38–57$ μs), which in MS lesion tissue decreases in size and possibly T_2 value (8–13 %, $T_2 = 26–73$ μs). Magic angle spinning spectroscopy in normal white matter showed lipid peaks which were considerably lower in grey matter and almost absent in MS tissue.

Clinically, this may be the time for the revival of PD. In Section 4.6 a range of clinical applications, related to increases in water content and to demyelination, were shown. Some clinical studies, measuring both PD and T_1, would identify whether PD will give useful information in disease, or whether T_1 measurements will be as informative (and easier to obtain). The role of myelin water measurements is likely to increase, although the poor coverage of current sequences will limit its use.

Acknowledgements

Gareth Barker, Declan Chard, Alex Mackay and Katherine Miszkiel provided helpful discussion. Chris Benton and Gerard Davies provided the images in Figure 4.1.

REFERENCES

Allen, P. S., Castro, M. E., Treiber, E. O., Lunt, J. A. and Boisvert, D. P. 1986, A proton NMR relaxation

evaluation of a model of brain oedema fluid, *Phys. Med. Biol.* **31**(7), 699–711.

Bakker, C. J., de Graaf, C. N. and van Dijk, P. 1984, Derivation of quantitative information in NMR imaging: a phantom study, *Phys. Med. Biol.* **29**(12), 1511–1525.

Beaulieu, C., Fenrich, F. R. and Allen, P. S. 1998, Multicomponent water proton transverse relaxation and T_2-discriminated water diffusion in myelinated and nonmyelinated nerve, *Magn. Reson. Imag.* **16**(10), 1201–1210.

Bell, B. A., Smith, M. A., Kean, D. M., McGhee, C. N., MacDonald, H. L., Miller, J. D., Barnett, G. H., Tocher, J. L., Douglas, R. H. and Best, J. J. 1987, Brain water measured by magnetic resonance imaging. Correlation with direct estimation and changes after mannitol and dexamethasone, *Lancet* **1**(8524), 66–69.

Bloom, M., Holmes, K. T., Mountfor, C. E. and Williams, P. G. 1986, Complete proton magnetic resonance in whole cells, *J. Magn. Reson.* **69**, 73–91.

Brix, G., Schad, L. R. and Lorenz, W. J. 1990, Evaluation of proton density by magnetic resonance imaging: phantom experiments and analysis of multiple component proton transverse relaxation, *Phys. Med. Biol.* **35**(1), 53–66.

Brooks, R. A., Di Chiro, G. and Keller, M. R. 1980, Explanation of cerebral white–gray contrast in computed tomography, *J. Comput. Assist. Tomogr.* **4**(4), 489–491.

Christiansen, P., Toft, P. B., Gideon, P., Danielsen, E. R., Ring, P. and Henriksen, O. 1994, MR-visible water content in human brain: a proton MRS study, *Magn. Reson. Imag.* **12**(8), 1237–1244.

Clare, S. and Jezzard, P. 2001, Rapid $T(1)$ mapping using multislice echo planar imaging, *Magn. Reson. Med.* **45**(4), 630–634.

Danielsen, E. R. and Henriksen, O. 1994, Absolute quantitative proton NMR spectroscopy based on the amplitude of the local water suppression pulse. Quantification of brain water and metabolites, *NMR Biomed.* **7**(7), 311–318.

Davie, C. A., Hawkins, C. P., Barker, G. J., Brennan, A., Tofts, P. S., Miller, D. H. and McDonald, W. I. 1993, Detection of myelin breakdown products by proton magnetic resonance spectroscopy, *Lancet* **341**(8845), 630–631.

Does, M. D. and Snyder, R. E. 1995, T_2 relaxation of peripheral nerve measured *in vivo*, *Magn. Reson. Imag.* **13**(4), 575–580.

Ernst, T., Kreis, R. and Ross, B. D. 1993, Absolute quantitation of water and metabolites in the human brain. I. Compartments and water, *J. Magn. Reson. Ser. B* **102**, 1–8.

Farace, P., Pontalti, R., Cristoforetti, L., Antolini, R. and Scarpa, M. 1997, An automated method for mapping human tissue permittivities by MRI in hyperthermia treatment planning, *Phys. Med. Biol.* **42**(11), 2159–2174.

Fatouros, P. P. and Marmarou, A. 1999, Use of magnetic resonance imaging for in vivo measurements of water content in human brain: method and normal values, *J. Neurosurg.* **90**(1), 109–115.

Fatouros, P. P., Marmarou, A., Kraft, K. A., Inao, S. and Schwarz, F. P. 1991, In vivo brain water determination by T_1 measurements: effect of total water content, hydration fraction, and field strength, *Magn. Reson. Med.* **17**(2), 402–413.

Fernandez-Seara, M. A., Song, H. K. and Wehrli, F. W. 2001, Trabecular bone volume fraction mapping by low-resolution MRI, *Magn. Reson. Med.* **46**(1), 103–113.

Fischer, H. W., Rinck, P. A., Van Haverbeke, Y. and Muller, R. N. 1990, Nuclear relaxation of human brain gray and white matter: analysis of field dependence and implications for MRI, *Magn. Reson. Med.* **16**(2), 317–334.

Gideon, P., Rosenbaum, S., Sperling, B. and Petersen, P. 1999, MR-visible brain water content in human acute stroke, *Magn. Reson. Imag.* **17**(2), 301–304.

Gutteridge, S., Ramanathan, C. and Bowtell, R. 2002, Mapping the absolute value of M0 using dipolar field effects, *Magn. Reson. Med.* **47**(5), 871–879.

Hoult, D. I. 2000, The principle of reciprocity in signal strength calculations – a mathematical guide, *Conc. Magn. Reson.* **12**, 173–187.

Hoult, D. I. and Richards, R. E. 1976, The signal-to-noise ratio of the nuclear magnetic resonance experiment, *J. Magn. Reson.* **24**, 71–85.

Just, M. and Thelen, M. 1988, Tissue characterization with T_1, T_2, and proton density values: results in 160 patients with brain tumors, *Radiology* **169**(3), 779–785.

Kaneoke, Y., Furuse, M., Inao, S., Saso, K., Yoshida, K., Motegi, Y., Mizuno, M. and Izawa, A. 1987, Spin-lattice relaxation times of bound water – its determination and implications for tissue discrimination, *Magn. Reson. Imag.* **5**(6), 415–420.

Kaye, G. W. C. and Laby, T. H. 1959, *Tables of Physical and Chemical Constants and Some Mathematical Functions*. Longmans, London.

Kreis, R. 1997, Quantitative localized 1 H MR spectroscopy for clinical use, *Prog. Nucl. Magn. Reson. Spectrosc.* **31**, 155–195.

Laule, C., Vavasour, I. M., Oger, J., Paty, D. W., Li, D. K. B. and MacKay, A. L. 2002, T_2 relaxation measurements of in-vivo water content and myelin water content in normal appearing white matter and lesions in multiple sclerosis, *Proc. Intl. Soc. Magn. Reson. Med.* **10**, 185.

Lerski, R. A., Straughan, K. and Orr, J. S. 1984, Calibration of proton density measurements in nuclear magnetic resonance imaging, *Phys. Med. Biol.* **29**(3), 271–276.

MacDonald, H. L., Bell, B. A., Smith, M. A., Kean, D. M., Tocher, J. L., Douglas, R. H., Miller, J. D. and Best, J. J. 1986, Correlation of human NMR T_1 values measured in vivo and brain water content, *Br. J. Radiol.* **59**(700), 355–357.

MacKay, A., Whittall, K., Adler, J., Li, D., Paty, D. and Graeb, D. 1994, In vivo visualization of myelin water in brain by magnetic resonance, *Magn. Reson. Med.* **31**(6), 673–677.

Marmarou, A., Poll, W., Shulman, K. and Bhagavan, H. 1978, A simple gravimetric technique for measurement of cerebral edema, *J. Neurosurg.* **49**(4), 530–537.

McLean, M. A., Woermann, F. G., Simister, R. J., Barker, G. J. and Duncan, J. S. 2001, *In vivo* short echo time ^{1}H-magnetic resonance spectroscopic imaging (MRSI) of the temporal lobes, *Neuroimage* **14**(2), 501–509.

Menon, R. S., Rusinko, M. S. and Allen, P. S. 1992, Proton relaxation studies of water compartmentalization in a model neurological system, *Magn. Reson. Med.* **28**(2), 264–274.

Nelson, S. R., Mantz, M. L. and Maxwell, J. A. 1971, Use of specific gravity in the measurement of cerebral edema, *J. Appl. Physiol.* **30**(2), 268–271.

Norton, W. T., Poduslo, S. E. and Suzuki, K. 1966, Subacute sclerosing leukoencephalitis. II. Chemical studies including abnormal myelin and an abnormal ganglioside pattern, *J. Neuropathol. Exp. Neurol.* **25**(4), 582–597.

Parker, G. J., Barker, G. J. and Tofts, P. S. 2001, Accurate multislice gradient echo T(1) measurement in the presence of non-ideal RF pulse shape and RF field nonuniformity, *Magn. Reson. Med.* **45**(5), 838–845.

Ramani, A., Aliev, A. E., Barker, G. J. and Tofts, P. S. 2001, Detection of ultra short T_2 species in human white matter by MAS NMR and multiexponential T_2 analysis, *International Society of Magnetic Resonance in Medicine 5th Meeting*, Vancouver, Vol **9**, p. 1359.

Roberts, D. A., Rizi, R., Lenkinski, R. E. and Leigh, J. S. Jr. 1996, Magnetic resonance imaging of the brain: blood partition coefficient for water: application to spin-tagging measurement of perfusion, *J. Magn. Reson. Imag.* **6**(2), 363–366.

Schepps, J. L. and Foster, K. R. 1980, The UHF and microwave dielectric properties of normal and tumour tissues: variation in dielectric properties with tissue water content, *Phys. Med. Biol.* **25**(6), 1149–1159.

Stanisz, G. J., Kecojevic, A., Bronskill, M. J. and Henkelman, R. M. 1999, Characterizing white matter with magnetization transfer and $T(2)$, *Magn. Reson. Med.* **42**(6), 1128–1136.

Stevenson, V. L., Parker, G. J., Barker, G. J., Birnie, K., Tofts, P. S., Miller, D. H. and Thompson, A. J. 2000, Variations in T_1 and T_2 relaxation times of normal appearing white matter and lesions in multiple sclerosis, *J. Neurol. Sci.* **178**(2) 81–87.

Stewart, W. A., MacKay, A. L., Whittall, K. P., Moore, G. R. and Paty, D. W. 1993, Spin-spin relaxation in experimental allergic encephalomyelitis. Analysis of CPMG data using a non-linear least squares method and linear inverse theory, *Magn. Reson. Med.* **29**(6), 767–775.

Takagi, H., Shapiro, K., Marmarou, A. and Wisoff, H. 1981, Microgravimetric analysis of human brain tissue: correlation with computerized tomography scanning, *J. Neurosurg.* **54**(6), 797–801.

Tofts, P. S. 1994, Standing waves in uniform water phantoms, *J. Magn. Reson. Ser. B* **104**, 143–147.

Torack, R. M., Alcala, H., Gado, M. and Burton, R. 1976, Correlative assay of computerized cranial tomography CCT, water content and specific gravity in normal and pathological postmortem brain, *J. Neuropathol. Exp. Neurol.* **35**(4), 385–392.

Tourtellotte, W. W. and Parker, J. A. 1968, Some spaces and barriers in postmortem multiple sclerosis, *Prog. Brain. Res.* **29**, 493–525.

Vavasour, I. M., Whittall, K. P., MacKay, A. L., Li, D. K., Vorobeychik, G. and Paty, D. W. 1998, A comparison between magnetization transfer ratios and myelin water percentages in normals and multiple sclerosis patients, *Magn. Reson. Med.* **40**(5), 763–768.

Venkatesan, R., Lin, W. and Haacke, E. M. 1998, Accurate determination of spin-density and T_1 in the presence of RF-field inhomogeneities and flip-angle miscalibration, *Magn. Reson. Med.* **40**(4), 592–602.

Venkatesan, R., Lin, W., Gurleyik, K., He, Y. Y., Paczynski, R. P., Powers, W. J. and Hsu, C. Y. 2000, Absolute measurements of water content using magnetic resonance imaging: preliminary findings in an in vivo focal ischemic rat model, *Magn. Reson. Med.* **43**(1), 146–150.

Waiter, G. D. and Lerski, R. A. 1991, The variation of proton density in agarose gels used as NMR test substances through the use of glass beads, *Phys. Med. Biol.* **36**(4), 541–546.

Wehrli, F. W., Breger, R. K., MacFall, J. R., Daniels, D. L., Haughton, V. M., Charles, H. C. and Williams, A. L. 1985, Quantification of contrast in clinical MR brain imaging at high magnetic field, *Invest. Radiol.* **20**(4), 360–369.

Whittall, K. P., MacKay, A. L., Graeb, D. A., Nugent, R. A., Li, D. K. and Paty, D. W. 1997, In vivo measurement of T_2 distributions and water contents in normal human brain, *Magn. Reson. Med.* **37**(1), 34–43.

Queries in Chapter 4:

Q1. As you have not updated the footnote numbers in sequential order we have changed. Please check
Q2. Not cited in text. Please check.